Microgravity Sci. Technol. (2011) 23:59–65
DOI 10.1007/s12217-010-9230-9

ORIGINAL ARTICLE

Numerical Simulation of Water Droplets Falling Near a Wall: Existence of Wall Repulsion

Ruquan Liang · Zhangqing Liao · Wen Jiang · Guangdong Duan · Jingyu Shi · Peng Liu

Received: 19 January 2010 / Accepted: 28 July 2010 / Published online: 14 August 2010

Abstract The numerical simulation has been carried out to investigate the motion of a droplet initially near a wall under gravity and confirm the existence of the wall repulsive force on the droplet. The numerical model is developed based on a mass conservation level set algorithm to capture the surface deformation of the droplet. The results show that the wall repulsive force on the droplet initially near the wall plays an important role in the droplet falling process, and the viscosity force affects the oscillatory trajectory of the falling droplet. In addition, the mutual repulsive effect between two droplets is also studied by settling symmetrically two droplets, and the oscillatory mechanism of droplet motion is discussed as well.

Keywords Droplet · Wall proximity · Wall repulsion · Deformation · Level set method

Introduction

Droplets formed in different devices are encountered frequently in wide range applications and research fields, such as foods, polymers, metallurgy, and atmosphere. Information about droplet deformation behavior can be critical to manipulate and control the relevant engineering processes where droplet deformation and breakup phenomena are involved. The droplet deformation behavior is influenced mainly by stresses acting on the droplet and by the material properties of the droplet as well as surrounding continuous phase, such as the viscosity of the droplet, the viscosity of the surrounding fluid phase, and the surface tension. The viscous force tends to deform the droplet, and the surface tension force works to restore the shape of the droplet. In addition, the apparatus itself may affect the droplet deformation such as the effect of the wall of the apparatus on the deformation of the droplet near the wall, and this kind of effect is investigated in the present work.

Many experimental works have been done, including the pioneering work of Taylor (1932), to investigate the deformation and eventually the breakup of droplets in diverse flow fields (Flumerfelt 1972; Rallison 1984; Bentley and Leal 1986; Stone and Leal 1989; Milliken and Leal 1991; Varanasi et al. 1994). Very recently, Gatne et al. (2009) investigated experimentally the effect of surfactant molecular mass transport on the normal impact and spreading of a droplet of its aqueous solution on dry horizontal substrates. They found that besides reagent bulk properties, dynamic surface tension, surface wettability, and droplet Weber number govern the transient impact-spreading-recoil phenomena. The role of dynamic surface tension is evident in comparisons of impact dynamics of droplets of different surfactant solutions with identical equilibrium surface tension and same Weber number. On the other hand, many numerical efforts on this subject have been conducted as well. Wilkes et al. (1999) investigated the dynamics of formation of a drop of a Newtonian liquid from a capillary tube into an

R. Liang (✉)
Key Laboratory of National Education Ministry for Electromagnetic Processes of Materials, Northeastern University, No.3-11, Wenhua Road, Shenyang 110004, China
e-mail: liang@epm.neu.edu.cn

Z. Liao · W. Jiang · G. Duan · J. Shi · P. Liu
Graduate School of Northeastern University, No.3-11, Wenhua Road, Shenyang 110004, China

ambient gas phase. Calculations have also been carried out to determine the range of parameters over which algorithms that treat the drop liquid as inviscid and the flow inside it as irrotational can accurately predict the dynamics of formation of drops of low viscosity liquids. Wilkes and Basaran (2001) studied the dynamics of a liquid drop which was supported on a solid rod that was forced to undergo large-amplitude, time-periodic oscillations along its axis using a computational approach based on the Galerkin/finite element method and an adaptive mesh generation technique which enables discretization of overturning interfaces and analysis of drop breakup. They found that the forcing amplitude and/or frequency can be chosen so as to prevent the formation of long liquid necks, which typically favor the formation of satellite droplets after breakup. Ni et al. (2006) presented a direct simulation of a droplet falling in a different background liquid and a variable time step method to improve conservation. Liang and Chen (2009) investigated the deformation dynamics of droplets under normal gravity and the Marangoni migration of droplets under microgravity.

The works on droplet dynamics under microgravity have also been done so far. Savino et al. (2001) studied numerically and experimentally the Marangoni effects responsible for a pushing force on a droplet interacting with a solid wall in the presence of a temperature gradient. Their results clarified questions of interest in the field of material science, in particular, they might provide some explanation for the minority phase separation observed during solidification processes under microgravity conditions. Savino et al. (2003) carried out an experimental and numerical analysis of the behavior of drops in a liquid matrix, in presence of temperature differences in preparation for a MAXUS sounding rocket flight to study wetting and coalescence prevention induced by thermal Marangoni effect. The theoretical-numerical study of the problem has been conducted with a thermo-fluidynamic model based on the assumption of the existence of a fluid film between the drop and the lower surface. Savino et al. (2004) reported the preliminary results of the microgravity experiment and a number of numerical simulations aimed at explaining and correlating the experimental findings in a microgravity experiment on droplets, wetting and coalescence prevention. The decreasing of the film thickness, as expected, was detected when the thermal gradient was reduced until wetting occurred at a "critical" temperature difference. Detailed reviews on numerical, experimental and modeling investigations of the deformation and breakup of droplets in simple and complex flow fields were given by Stone (1994), Briscoe et al. (1999).

Despite the fact that a number of papers touched upon droplet deformation, it is yet not fully known the effect of the wall on the moving droplet near the wall. In this paper, we will present such a study using a mass conservation level set approach to investigate the deformation and breakup of the droplet initially near a wall under gravity.

Equations of Motion

In our investigation, an initially circular droplet with radius R is centered at (a, b) and surrounded by the gas phase under gravity in a rectangular container with height L_y and width L_x as shown in Fig. 1. The equations of motion for an incompressible flow are given by the following dimensionless Navier-Stokes equations, which include gravitational as well as viscosity and surface tension effects.

$$\nabla \cdot \mathbf{u} = 0 \tag{1}$$

$$\mathbf{u}_t + (\mathbf{u} \cdot \nabla)\,\mathbf{u} = \mathbf{g}_u + \frac{1}{\rho}\left(-\nabla p + \frac{1}{\mathrm{Re}}\nabla \cdot (2\mu \mathbf{D}) + \frac{1}{\mathrm{We}}\kappa\delta\,(d)\,\mathbf{n}\right) \tag{2}$$

where $\mathbf{u} = (u, v)$ is the fluid velocity, $\rho = \rho(\mathbf{x}, t)$ is the fluid density, $\mu = \mu(\mathbf{x}, t)$ is the fluid viscosity, $\mathbf{D}$ is the viscous stress tensor, κ is the curvature of the interface, δ is the Dirac delta function, d is the normal distance to the interface, $\mathbf{n}$ is the unit normal vector at the interface, t is the time, p is the pressure, $\mathbf{g}_u$ represents the unit gravitational force. The dimensionless parameters used are Reynolds number and Weber number defined as $\mathrm{Re} = \frac{(L)^{3/2}\sqrt{g}\rho_l}{\mu_l}$ and $We = \frac{(L)^2 g\rho_l}{\sigma}$, respectively. Here ρ_l and μ_l are the dimensional liquid density and viscosity, respectively, σ is the surface tension, L is the characteristic length, $L = 2R$, R is the initial radius of the circular droplet, the characteristic velocity $U_\infty = \sqrt{2Rg}$, g is the gravitational acceleration, and the characteristic time $\bar{t} = \sqrt{2R/g}$.

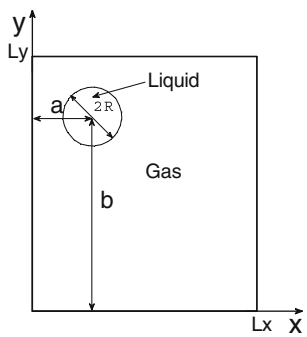

Fig. 1 The schematic diagram of the droplet motion model

Numerical Method

Level Set Function and Its Formulation

The level set method was originally introduced by Osher and Sethian (1988) to numerically predict the moving interface $\Gamma(t)$ between two fluids. Instead of explicitly tracking the interface, the level set method implicitly captures the interface by introducing a smooth signed distance from the interface in the entire computational domain. The level set function $\phi(\mathbf{x}, t)$ is taken to be positive outside the interface, zero on the interface and negative inside the surface. The interface motion is predicted by solving the following convection equation for the level set function of $\phi(\mathbf{x}, t)$ given by,

$$\phi_t + \mathbf{u} \cdot \nabla\phi = 0 \tag{3}$$

The density ρ and viscosity μ in the flow field can then be expressed as follows.

$$\rho(\phi) = 1 + \left(\rho_g/\rho_l - 1\right) H_\alpha(\phi) \tag{4}$$

$$\mu(\phi) = 1 + \left(\mu_g/\mu_l - 1\right) H_\alpha(\phi) \tag{5}$$

$$H_\alpha(\phi) = \begin{cases} 0 & \phi < -\alpha \\ (\phi + \alpha)/(2\alpha) + \sin(\pi\phi/\alpha)/2\pi & |\phi| \le \alpha \\ 1 & \phi > \alpha \end{cases} \tag{6}$$

where subscripts g and l denote the gas and liquid phases, respectively, and α is the prescribed thickness of the interface, while we used $\alpha = \Delta x/2$ in this work, here Δx is the grid spacing. Sussman et al. (1994) proposed an iterative procedure to reinitialize the level set function after solving the convection equation for the level set function.

$$\phi_t = \frac{\phi_0}{\sqrt{\phi_0^2 + (\Delta x)^2}} (1 - |\nabla\phi|) \tag{7}$$

$$\phi(\mathbf{x}, 0) = \phi_0(\mathbf{x}) \tag{8}$$

where $\phi_0(\mathbf{x})$ has the same zero level set as $\phi(\mathbf{x})$.

In fact, the numerical discretization of the level set formulation does not guarantee the mass conservation. To overcome this difficulty, a mass conserving procedure must be carried out by solving the following area compensation equation to a steady state,

$$\frac{\partial\phi}{\partial t} + \left[1 - \frac{A(t)}{A_0}\right] F(\kappa) |\nabla\phi| = 0 \tag{9}$$

where $A(t)$ is the liquid phase area at time t corresponding to the level set function $\phi(t)$, A_0 is the initial area of the liquid phase for the initial condition, $F(\kappa)$ is defined as follow,

$$F(\kappa) = 1.0 + h\kappa^n \tag{10}$$

The $F(\kappa)$ is an area constraint function and can be considered as a function of the local curvature, which varies with h and n. The procedure converges much faster when $h = 0$ and $n = 0$, which are used in the present calculation. We stop the procedure when the relative error between $A(t)$ and A_0 is less than 10^{-5}.

Boundary, Initial and Numerical Conditions

In the gas-liquid system studied here, the initially stationary droplet and the background phase are considered with the initial condition

$$\mathbf{u}(t = 0) = 0 \tag{11}$$

The non-slip condition is used at the four wall boundaries of the closed channel

$$\mathbf{u} = 0 \tag{12}$$

The present strategy is further summarized below. The level set formulation of Eulerian interface capturing methods is applied to analyze the free surface motion of the droplet. The Navier-Stokes equations in primitive variable formulations are solved on a staggered grid by the method of lines. The advection terms are discretized by the quadratic upstream interpolation for convective kinematics (QUICK) method (Leonard 1979) and the other terms by the central finite difference method except for the body force, and a second-order Adams-Bashforth method (Gear 1971) is used as the time integration scheme. The Poisson equations are solved by means of the successive over relaxation (SOR) approach (Rigal 1987). The continuum surface force (CSF) model (Brackbill et al. 1992) is employed to treat the surface tension force at the interface.

Results and Discussion

The code validation has been carried out by comparing present results with those of van der Pijl et al. (2005) for a droplet falling under gravity. The stationary droplet in air is considered initially. The non-dimensional sizes include: $L_x = 6R$, $L_y = 9R$, $a = 3R$, $b = 6R$, $R = 0.5$ and the dimensional size is $\overline{L_x} = 0.02$ m. The gravity is $g = 9.8$ m/s^2, and the material constants include:

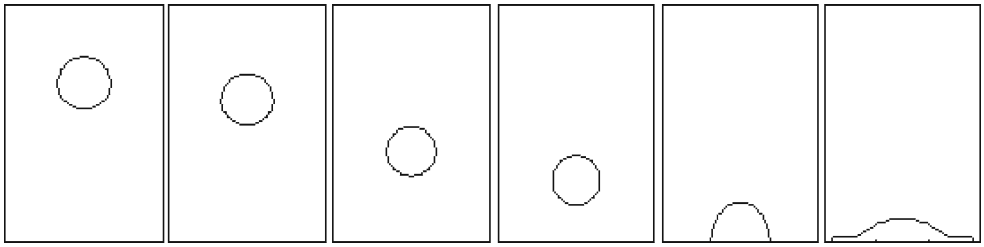

Fig. 2 Interface positions for the falling droplet at several times (*from left to right* $t = 0.0$ s, $t = 0.02$ s, $t = 0.04$ s, $t = 0.05$ s, $t = 0.06$ s, $t = 0.065$ s)

$\sigma = 0.0728$ kg/s^2, $\rho_l = 10^3$ kg/m^3, $\rho_g = 1.226$ kg/m^3, $\mu_l = 1.137 \times 10^{-3}$ kg/ms, $\mu_g = 1.78 \times 10^{-5}$ kg/ms, respectively. The results from the present work are shown in Fig. 2 showing the interface positions and shapes at several times for the falling droplet, which compare well with ones of van der Pijl et al. at every time step (see Fig. 12 of van der Pijl et al. (2005)). Note that all results presented in this paper are shown in dimensionless forms except for the droplet falling times shown in Fig. 2.

1. Single droplet motion

An initially stationary circular droplet of radius R is released from a position at $(1.5R, 16.5R)$ in a rectangular channel with the width L_x and height L_y, and the droplet is heavier than the surrounding fluid. The non-dimensional sizes are: $L_x = 9R$, $L_y = 18R$, $R = 0.5$. The simulation is conducted with a set of parameters, Re = 100, We = 50, $\rho_l/\rho_g = 1.25$, $\mu_l/\mu_g = 100$. Once the simulation starts, the droplet will fall down under the effect of gravity. Figure 3a presents the droplet surface profiles between t = 0.0 and t = 37.5 with time interval 2.5, and the velocity field and droplet shape at t = 37.5 is shown in Fig. 3b. The viscosity force tends to deform the droplet, and the surface tension force works to maintain the shape of the droplet when the droplet moves down in a lighter fluid. The near wall also has a wall repulsive effect on the moving droplet by applying a repulsive force on the droplet, which tends to deform the droplet as well and pushes the droplet away from the wall. Under such complicated effects, the droplet moves towards the center of the channel. As the droplet deforms, the positions of its mass center are changed consecutively, which results in a vibration force. At the same time, the droplet falling movement also induces a pressure different around the droplet. As the droplet is away from the left wall, the wall repulsive force decreases, while the pressure difference and the vibration force push the droplet back to the left wall. The process is repeated and the droplet undergoes an oscillatory trajectory when it moves down under gravity. Figure 3b clearly illustrates the oscillatory vortex sheet in the velocity field for the falling movement of the droplet near the wall, which confirms the oscillation of the droplet movement as well. Figure 3c illustrates the nearest and farthest distances between the droplet and the left wall of the channel, which shows further the oscillatory motion of the droplet.

Next, the effect of Re number on the droplet movement is observed by setting different Re number. Figure 4 illustrates the droplet surface profiles between t = 0.0 and t = 60.0 with time interval 2.5 for the case of Re = 10 and the other computational conditions are kept the same with those in Fig. 3. As the Re

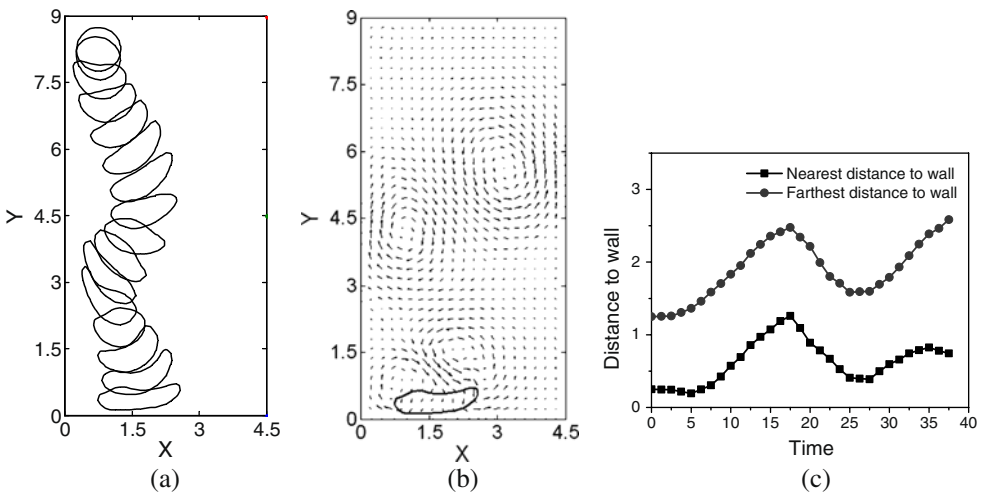

Fig. 3 A falling droplet initially near the left wall at $(1.5R, 16.5R)$ for Re = 100, We = 50, $\rho_l/\rho_g = 1.25$, $\mu_l/\mu_g = 100$, $R = 0.5$. (**a**) Droplet surface profiles, (**b**) velocity field at $t = 37.5$, and (**c**) the nearest and farthest distances between the droplet and the left wall of the channel

number decreases, the inertia effect decreases and it takes a longer time for the droplet to move down from the initial position to the bottom of the channel. The droplet undergoes a larger deformation owing to the strong viscous damping in a long time falling movement for the low Re number case of Re = 10, and the droplet breaks up eventually as shown in Fig. 4b. Moreover, the oscillatory frequency decreases remarkably as the Re number is decreased. The density of the background fluid is close to that of the droplet, thus the droplet falls actually in a lighter liquid. Because the inertia force of the droplet motion is small, once the droplet approaches the left wall enough, the wall repulsive force increases so that it is larger enough than the pressure difference and the vibration force, which can push the droplet away from the wall. Therefore, the droplet falls and splits into a main droplet and small ones without any contact with the wall.

In order to study the effect of initial position of the droplet on the droplet motion, the droplet is released from a position of $(4.5R, 16.5R)$, and the other computational conditions are kept the same with those in Fig. 4. The droplet surface profiles between t = 0.0 and t = 80.0 with time interval 2.5 are shown in Fig. 5a, and the velocity field and the droplet shapes at t = 80.0 are shown in Fig. 5b. The droplet is located at the center of the channel and falls straight along the centerline without lateral motion since there is no wall repulsive force acting on the droplet to produce appreciable oscillation as found in Figs. 3 and 4 before the droplet is broken. As the droplet deforms largely and breaks into two small droplets, the pressure difference and the

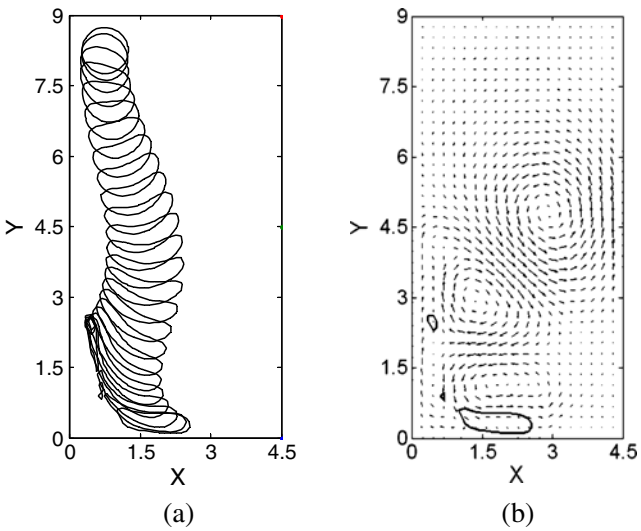

Fig. 4 A falling droplet initially near the left wall at $(1.5R, 16.5R)$ for Re = 10, We = 50, $\rho_l/\rho_g = 1.25$, $\mu_l/\mu_g = 100$, $R = 0.5$. (**a**) Droplet surface profiles and (**b**) the velocity field at $t = 60.0$

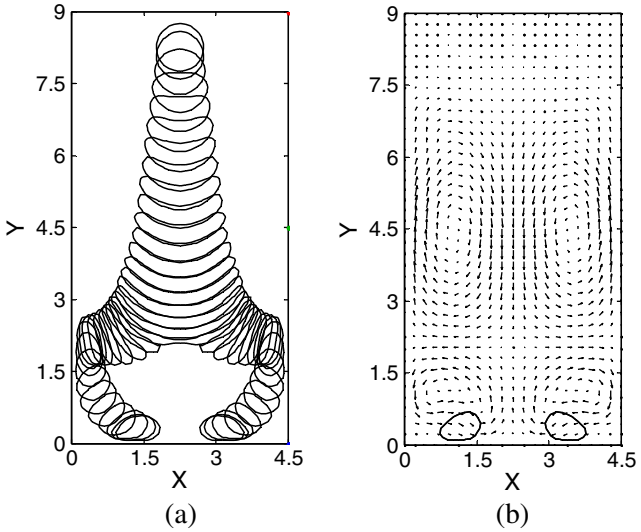

Fig. 5 A falling droplet initially in the central region at $(4.5R, 16.5R)$ for Re = 10, We = 50, $\rho_l/\rho_g = 1.25$, $\mu_l/\mu_g = 100$, $R = 0.5$. (**a**) Droplet surface profiles and (**b**) the velocity field at $t = 80.0$

vibration force push the two droplets to move towards the left and right walls, respectively. When they are near the left and right walls enough, the repulsive forces from the two walls push them away from the two walls, respectively.

The vertical side walls of the channel are regarded as the regular walls, and the other kind of side walls of the channel are regarded as the irregular walls. The effect of the irregular wall on the droplet motion is also checked. An initially stationary circular droplet of radius R is released from a position at $(6R, 16.5R)$ in an irregular channel with inclined left and right walls under gravity. The non-dimensional sizes are: $L_x = 12R$, $L_y = 18R$, $R = 0.5$. The simulation is conducted with a set of parameters, Re = 100, We = 50, $\rho_l/\rho_g = 1.25$, $\mu_l/\mu_g = 100$. The droplet surface profiles between t = 0.0 and t = 37.5 with time interval 2.5 are shown in Fig. 6a. When the droplet is released from the initial position, it falls down due to the effect of gravity. At the same time, the near distance between the droplet and the right wall results in a repulsive force which pushes the droplet away from the right wall. As the droplet approaches the left wall, the repulsive force coming from the left wall keeps the droplet apart from the left wall. Therefore, the droplet undergoes an oscillatory process as it falls down. The oscillatory process can be found from the oscillatory vortex sheet in the velocity field for the falling movement of the droplet at t = 37.5 (Fig. 6b). In Fig. 7, an initially stationary circular droplet of radius R is released from a position $(3R, 16.5R)$ in an irregular channel with an oval left wall under gravity, and the other computational conditions are kept the same with

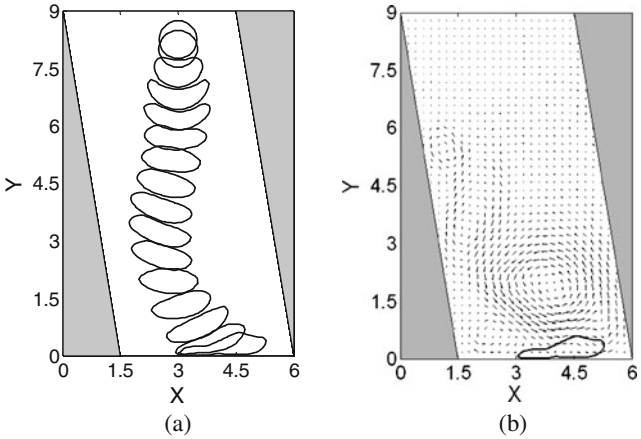

Fig. 6 A falling droplet initially near the right wall at $(6R, 16.5R)$ for Re = 100, We = 50, $\rho_l/\rho_g = 1.25$, $\mu_l/\mu_g = 100$, $R = 0.5$. (**a**) Droplet surface profiles and (**b**) the velocity field at $t = 37.5$

those in Fig. 6. The droplet experiences an obvious oscillation in its falling process (Fig. 7a), and the droplet is broken when it is pushed back to the left wall. The small part of the broken droplet is well reserved as shown in Fig. 7b, which shows that the mass conservation is well done attributing to the area compensation in the level set method.

2. Double droplet motion

Finally, the interaction between two droplets is also investigated by settling two droplets symmetrically in the computational regions with same initial horizontal positions at $(3R, 16.5R)$ and $(6R, 16.5R)$, respectively. The simulation is conducted with We = 25, and the other computational conditions are kept the same with those in Fig. 3. The shape development of the falling

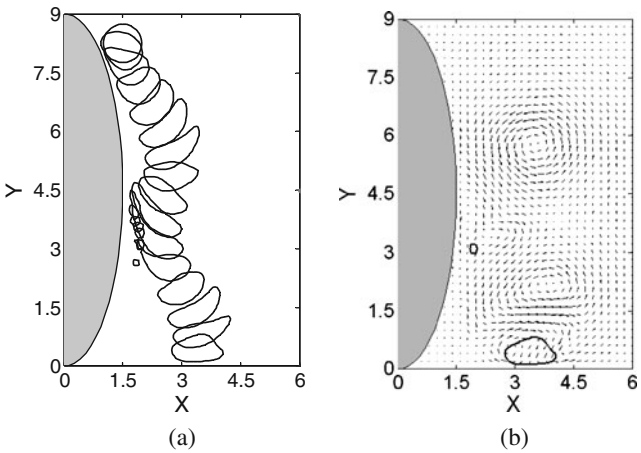

Fig. 7 A falling droplet initially near the left wall at $(3R, 16.5R)$ for Re = 100, We = 50, $\rho_l/\rho_g = 1.25$, $\mu_l/\mu_g = 100$, $R = 0.5$. (**a**) Droplet surface profiles and (**b**) the velocity field at $t = 37.5$

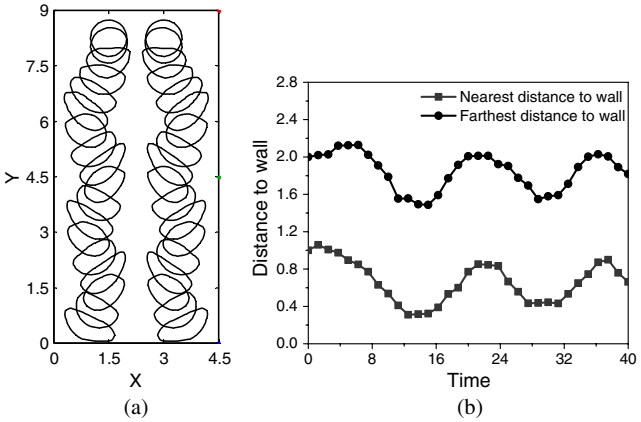

Fig. 8 Two falling droplets settling symmetrically with same initial horizontal positions at $(3R, 16.5R)$ and $(6R, 16.5R)$, respectively, for Re = 100, We = 25, $\rho_l/\rho_g = 1.25$, $\mu_l/\mu_g = 100$, $R = 0.5$. (**a**) Droplet surface profiles and (**b**) the nearest and farthest distances between the left droplet and the left wall of the channel

droplet between t = 0.0 and t = 42.5 with time interval 2.5 is shown in Fig. 8a. Initially, the mutual repulsion for the two droplets keeps them apart and forces them to move towards the two side walls, respectively, and then the two walls tend to push the two droplets together when the two droplets close to the two walls, respectively. Therefore, the two droplets exhibit oscillatory motion as shown in Fig. 8a. The nearest and farthest distances between the left droplet and the left wall of the channel are shown in Fig. 8b. The nearest and farthest distances vibrate in the form of sinusoidal function, which confirms further the oscillatory motion of the left droplet.

Conclusions

The wall effect on the falling droplet initially near the wall under gravity is investigated numerically using the mass conserving level set approach to study the deformation mechanisms of the falling droplet. From this work, the following conclusions can be drawn.

1. When the droplet initially near a wall moves down in a lighter fluid, the near wall has a wall repulsive effect on the droplet by applying a repulsive force on the droplet, which tends to deform the droplet and pushes the droplet away from the wall. As the droplet deforms, the positions of its mass center are changed consecutively, which results in a vibration force. At the same time, the droplet falling movement also induces a pressure different around the droplet. As the droplet is away from the wall, the wall repulsive force decreases and the pressure

difference and the vibration force push the droplet back to the wall. The process is repeated and the droplet undergoes an oscillatory trajectory, and the oscillatory vortex sheet of the droplet confirms the oscillation of the droplet movement and the existence of the wall repulsion effect.

2. For the low Re number case, the droplet undergoes a larger deformation owing to the viscous damping in a long falling time and breaks up eventually, and the oscillatory frequency decreases remarkably as the Re number is decreased. The small part of the broken droplet is well reserved in the computation for droplet breaking cases, which shows that the mass conservation is well done attributing to the area compensation in the level set method. The results for the double droplet motion illustrate the existence of the mutual repulsion between the two droplets.

References

Bentley, B.J., Leal, L.G.: A computer-controlled four-roll mill for investigations of particle and drop dynamics in two-dimensional linear shear flows. J. Fluid Mech. **167**, 219–240 (1986)

Brackbill, J.U., Kothe, D.B., Zemach, C.: A continuum method for modeling surface tension. J. Comput. Phys. **100**(2), 335–354 (1992)

Briscoe, B.J., Lawrence, C.J., Mietus, W.G.P.: A review of immiscible fluid mixing. Adv. Colloid Interface Sci. **81**, 1–17 (1999)

Flumerfelt, R.W.: Drop breakup in simple shear fields of viscoelastic fluids. Ind. Eng. Chem. Fundam. **11**, 312–318 (1972)

Gatne, K.P., Jog, M.A., Manglik, R.M.: Surfactant-induced modification of low Weber number droplet impact dynamics. Langmuir 25(14), 8122–8130 (2009)

Gear, W.C.: Numerical initial value problems in ordinary differential equations. Prentice-Hall, Inc. (1971)

Leonard, B.P.: Stable and accurate convective modeling procedure based on quadratic upstream interpolation. Comput. Methods Appl. Mech. Eng. **19**(1), 59–98 (1979)

Liang, R.Q., Chen, Z.: Dynamics for droplets in normal gravity and microgravity. Microgravity Sci. Technol. **21**, 247–254 (2009)

Milliken, W.J., Leal, L.G.: Deformation and breakup of viscoelastic drops in planar extensional flows. J. Non-Newton Fluid Mech. **40**, 355–379 (1991)

Ni, M.J., Komori, S., Morley, N.B.: Direct simulation of falling droplet in a closed channel. Int. J. Heat Mass Transfer **49**, 366–376 (2006)

Osher, S., Sethian, J.A.: Fronts propagating with curvature-dependent speed: algorithms based on Hamilton–Jacobi formulations. J. Comput. Phys. **79**(1), 12–49 (1988)

Rallison, J.M.: The deformation of small viscous drops and bubbles in shear flows. Ann. Rev. Fluid Mech. **16**, 45–66 (1984)

Rigal, A.: SOR methods for coupled elliptic partial differential equations. J. Comput. Phys. **71**(1), 181–193 (1987)

Savino, R., Monti, R., Alterio, G.: Drops pushing by Marangoni forces. Phys. Fluids **13**(5), 1513–1516 (2001)

Savino, R., Nota, F., Fico, S.: Wetting and coalescence prevention of drops in a liquid matrix. Ground and parabolic flight results. Microgravity Sci. Technol. **14**(3), 3–12 (2003)

Savino, R., Monti, R., Nota, F., Fortezza, R., Carotenuto, L., Piccolo, C.: Preliminary results of the sounding rocket experiment on wetting and coalescence prevention by Marangoni effect. Acta Astronaut. **55**(3–9), 169–179 (2004)

Stone, H.A.: Dynamics of drop deformation and breakup in viscous fluids. Annu. Rev. Fluid Mech. **26**, 65–102 (1994)

Stone, H.A., Leal, L.G.: The influence of initial deformation on drop breakup in subcritical time-dependent flows at low Reynolds number. J. Fluid Mech. **206**, 223–263 (1989)

Sussman, M., Smereka, P., Osher, S.: A level set approach for computing solutions to incompressible two-phase flow. J. Comput. Phys. **114**, 146–159 (1994)

Taylor, G.I.: The viscosity of a fluid containing small drops of another fluid. Proc. R. Soc. Lond. Ser. A. **138**, 41–48 (1932)

van der Pijl, S.P., Segal, A., Vuik, C., Wesseling, P.: A mass-conserving level-set method for modelling of multi-phase flows. Int. J. Numer. Methods Fluids **47**, 339–361 (2005)

Varanasi, P.P., Ryan, M.E., Stroeve, P.: Experimental-study on the breakup of model viscoelastic drops in uniform shear-flow. Ind. Eng. Chem. Res. **33**, 1858–1866 (1994)

Wilkes, E.D., Basaran, O.A.: Drop ejection from an oscillating rod. J. Colloid Interface Sci. **242**(1), 180–201 (2001)

Wilkes, E.D., Phillips, S.D., Basaran, O.A.: Computational and experimental analysis of dynamics of drop formation. Phys. Fluids **11**(12), 3577–3598 (1999)